

RETRIEVALS OF ICE-WATER CONTENT FROM AN AIRBORNE ELASTIC LIDAR IN TROPICAL CONVECTIVE CLOUDS

Konstantin Baibakov^{1*}, Mengistu Wolde¹, Cuong Nguyen¹, Alexei Korolev², Ivan Heckman²

¹*Flight Research Laboratory, National Research Council (NRC), Ottawa, Canada,*

**Konstantin.Baibakov@nrc-cnrc.gc.ca*

²*Environment and Climate Change Canada (ECCC), Toronto, Canada*

ABSTRACT

Ice water content (IWC) is one of the critical parameters in determining the cloud radiative impact. In this work lidar-based IWC retrievals obtained in tropical mesoscale convective systems are evaluated in the context of an extensive in-situ and remote sensing instrumentation suite. Based on a test case of May 27, 2015 lidar-derived IWC values at 50 m above the aircraft were on average within 25% of the in-situ IWC measurements obtained using an isokinetic probe.

1 INTRODUCTION

Ice and mixed-phase clouds cover roughly 25% of the Earth's surface and can have a significant and variable effect on the Earth's radiation budget [1]. The ice water content (IWC), is one of the critical parameters in determining the cloud radiative impact and hydrological cycle. In addition, high IWC conditions are recognized by aviation authorities as potentially dangerous for operation of commercial aviation [2]. A substantial effort has been expended to estimate IWC from various in-situ and remote sensing measurements. In particular, several works have previously shown the feasibility of IWC retrievals from lidar extinction profiles, especially in relation to spaceborne lidars. However, in many cases this technique is applied to mid-latitude clouds with IWC values on the order of mg/m^3 . We have found no works that evaluate the potential of lidar IWC retrievals in the high ice water content (HIWC) environment, with IWC values reaching as high as 2-3 g/m^3 . Furthermore, the quality of the remotely sensed IWC measurements is often evaluated through comparisons with in-situ data. This can turn out to be problematic in HIWC, because the standard measurement techniques of estimating IWC, either from 2D particle imagery or hot-wire probes, can suffer from numerous instrumental issues [3]. Recently developed

isokinetic probes (IKP) [4] were designed to solve most of these issues and can provide accurate measurements at high IWC concentrations (up to 15 g/m^3) and air speeds (up to 200 m/s) [idem]. In May 2015, the NRC Convair-580 aircraft participated in the HAIC (High Altitude Ice Crystals)-HIWC project from an operational base in Cayenne (French Guiana, $5^\circ\text{N } 52^\circ\text{W}$). The project was aimed at better understanding of the HIWC environment with an eye towards reducing the dangers of flying in ice crystals icing (ICI) conditions. The Convair was jointly equipped by NRC and ECCC and included state of the art in-situ and remote sensing instrumentation. In particular, two quasi-identical Airborne Elastic Cloud Lidar systems (AECL-zenith and AECL-nadir) were installed onboard the Convair and acquired close to 40 hours of data. An IKP probe was also used during the campaign. The purpose of this paper is to briefly describe the AECL lidar system, discuss the AECL performance and evaluate AECL capabilities in supplying IWC information as compared to in-situ measurements. Section 2 describes the instrumentation and data processing with a focus on AECL. Section 3 presents the main results of the AECL-based IWC retrievals based on a representative test case of May 27, 2015. Finally, Section 4 summarizes our preliminary findings.

2 METHODS AND INSTRUMENTATION

2.1 AECL lidar description and data processing

Airborne Elastic Cloud Lidar (AECL) built by Alpenglow Instruments, LLC. is a compact airborne elastic lidar operating at 355nm. The lidar design is shown in Figure 1. AECL features a rotatable beam bender section that allows the instrument to be configured in either zenith or nadir orientation. The change in configuration, however, can not be performed while in-flight.

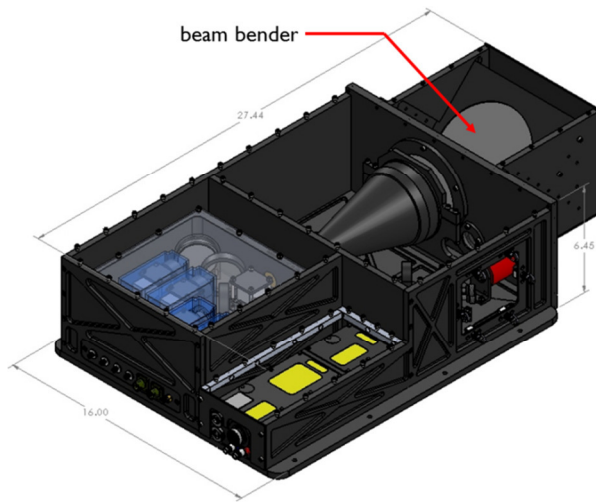


Figure 1. AECL design with a rotatable beam bender

AECL can estimate a degree of particle-induced depolarization of the emitted laser pulse by separately measuring parallel and perpendicular polarization components of the return signal, P_{\parallel} and P_{\perp} . The (linear) depolarization ratio, $LDR = P_{\perp} / P_{\parallel}$, can often provide an insight into the types of particles encountered by the laser beam with lower LDR values often associated with spherical (liquid) drops.

Table 1 Technical specifications of the AECL transmitter, receiver and data acquisition system

Transmitter	
Laser Wavelength	355nm YAG
Pulse Repetition Frequency	20 Hz
Pulse Width	≈8 ns
Pulse Energy	12mJ
Beam Divergence	0.4×10^{-3} radians
Receiver	
Diameter	≈100 mm
Field of View	≈1000 μrad
Data System	
Number of Channels	Four: Low and high gain parallel and perpendicular signals
Detector	PMT
Range Resolution	1.5m, 3.0m, 6.0m, 12m (programmable)

The essential AECL technical specifications are listed in Table 1 while the lidar data processing chain is briefly described below. First, the return

signal is background- and range-corrected to compensate for parasite (internal) signal sources and the R^2 signal drop off with range, respectively. Then the incomplete overlap correction is also applied to compensate for the effect of the laser beam not being entirely within the telescope FOV at the lowest ranges. We estimate that the full overlap is achieved at 150 m. Comparing the AECL results in the few lowest range bins against the in-situ (flight-level) data requires careful consideration of the incomplete overlap problem. In this work, we have used the method of [5] to correct the signal below 150 m by using calibration data in clear air. Despite the correction, we acknowledge that evaluating lidar data in the overlap region can be problematic and associated with a source of error. Once all the basic corrections have been applied, the lidar vertically resolved extinction coefficients are derived using a Klett technique with a boundary condition in the far range. This method requires an assumption of the particulate extinction-to-backscatter (or lidar) ratio, LR. In this work we used a constant vertically averaged value of $LR=20$ Sr consistent with climatological values from satellite statistics and other works. Only the lidar profiles in zenith direction were used for Klett inversions. Finally, once the extinction coefficient (κ) profiles have been computed, IWC profiles can be calculated using a power law parametrization:

$$IWC = a\kappa^b \quad (1)$$

where we used the values of $a=527$ and $b=1.32$ as per [1].

2.2 In-situ instrumentation

During the campaign, Convair-580 carried a multitude of in-situ instruments designed for cloud studies. Among them were particle imaging probes (including SPEC 2D-S and DMT PIP) as well as IKP for bulk IWC measurements. The imaging probes provide a visual information on particle size and shape. Particle probes' data was also used to derive cloud extinction coefficient and particle median mass size and concentration. IWC information can also be derived from imaging probes using empirical size-to-mass parameterization. The IKP provides reliable measurements of IWC by measuring a change in

absolute humidity from continuously aspirating and evaporating all encountered particles and ensuring that the air speed at the probe inlet matches the free stream air speed [3].

2.3 NAWX radar

The NAWX radar system [6] has polarimetric and Doppler capabilities at both frequencies (X-band: 9.41 GHz [3.2 cm], W-band: 94.05 GHz [3.2 mm]) and can switch electronically between zenith, nadir and side looking antennas. The equivalent radar reflectivity (Z_e) is used to characterize cloud structures in ice environments.

3 RESULTS

Figure 2 shows a dataset obtained on May 27, 2015 between 11:08 and 11:17 during the HAIC-HIWC flight campaign. Listed from top to bottom are: 1) lidar backscatter power (arbitrary units), 2) lidar depolarization (arbitrary units), 3) lidar extinction coefficient profiles obtained from Klett inversion (km^{-1} , log-scale), 4) radar W-band reflectivity (dBZ), 5) computed particle concentration, L^{-1} , 6) computed particle median diameter, μm , 7) extinction coefficient from in-situ data and lidar extinction at 50 m above aircraft (km^{-1}), 8) IWC measured by IKP and lidar-based IWC taken at 50 m above aircraft (g/m^3). White line in panes 1 and 4 signifies the last bin below which lidar returns are considered too weak to be used for data analysis. Figure 2 is a typical measurement scene from the HAIC-HIWC campaign and contains several features of interest relevant to AECL performance. The aircraft stayed at an altitude of ~ 5.5 km between 11:08 and 11:10 and then gradually ascended to 6 km by 11:17. Before 11:12:30 AECL penetration range is relatively high which allows the detection of multiple cloud layers up to 1.5 km above the aircraft. Lidar data indicates the presence of liquid droplets (high backscatter and low depolarization ratio) above 6 km with layers of glaciated particles (low backscatter and high depolarization ratio) immediately below. The time after 11:12:30 is associated with significantly reduced lidar penetration range and can be subdivided into the following relevant time periods (TP): TP1 (11:12:00-11:12:30), TP2 (11:13:05-11:13:45) and TP3 (11:13:45-11:16:30).

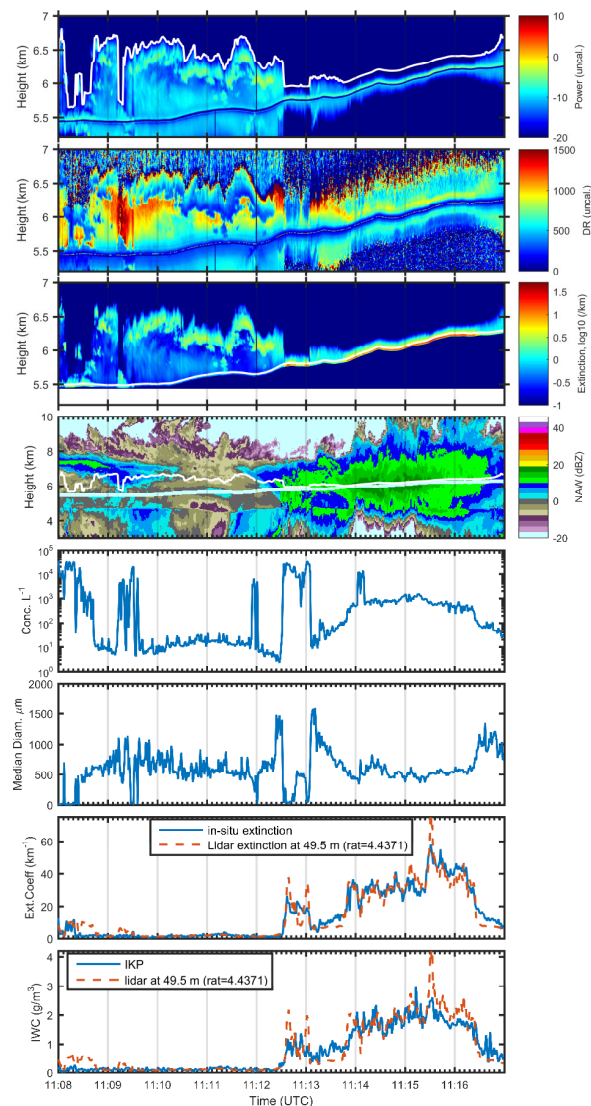


Figure 2 Lidar, radar and in-situ responses during the HAIC-HIWC on May 27, 2015. See text for details.

While TP1 and TP3 are both associated with relatively high lidar extinction values (reaching values $>20 \text{ km}^{-1}$), in-situ measurements show that the extinction is caused by different types of particles. Referring to panes 5 and 6 of Figure 2, it can be seen that particle concentrations are an order of magnitude higher during TP1 than during TP3 (10^3 vs 10^4 L^{-1}). At the same time, the particle median mass diameter, MMD, defined as the size that splits the mass size distribution into two parts equal by mass, gets as low as 50-60 μm during TP1 but stays at an average value of $\sim 500 \mu\text{m}$ during TP3. These observations imply that TP1 is dominated by small liquid cloud droplets, while TP3 consists of larger glaciated particles.

The Cloud Imaging Probe (CPI) imagery (not shown) corroborates this analysis, showing small regular particles during TP1 and predominantly unrimed columns during TP3. TP3 is associated with the High Ice Water Content environment – a primary subject of investigation in the campaign. Previous results show (e.g. [7]) that MMD in HIWC varies between 200 and 500 μm and decreases with increasing TWC and/or decreasing temperature. These statistics are consistent with the results of Figure 2. During TP3, lidar penetration range is significantly reduced from ~1.2 km at 11:10:35 to ~200m at 11:15:00. The occurrence of HIWC is also characterized by strong W-band radar reflectivity of up to 17 dBZ. The extinction pane of Figure 2 presents the in-situ extinction estimated from the particle size distribution as well as Klett-derived extinction taken at ~50 m above the aircraft and scaled by 4.44. Throughout the campaign Klett-derived extinction profiles had to be generally scaled by a factor of ~4 to match the in-situ extinction. While the source of this discrepancy is currently being investigated, low lidar extinction values can be explained, in part, by insufficient overlap and multiple scattering corrections as well as errors in the initial parameters used in Klett inversions, especially the cloud lidar ratio. It's clear nevertheless that relative variations in lidar extinction match well those from the in-situ based retrievals with $R^2=0.86$ for the entire time period between 11:12:30 and 11:17:00. Lidar extinction values were then used in Eq. (1) to derive IWC concentrations. Pane 8 shows a comparison between the IWC time-series derived from the IKP probe (IWC_{IKP}) and AECL-based IWC values taken at 50 m above aircraft (IWC_{lid}). During TP3 IWC_{lid} values were on average within 25% of the IWC_{IKP} and generally matched well the IWC_{IKP} in terms of relative variations.

4 CONCLUSIONS

In May 2015 AECL sampled regions of HIWC near Cayenne (French Guiana) with IWC values as high as 2-3 g/m^3 . Lidar IWC values derived from extinction using a power law parametrization were on average within 25% of the IKP measurements. The relatively good agreement is important for a number of reasons. First, a consistency between fundamentally different

instruments yields more credence to both the absolute values and the relative variations of IWC in the HIWC environment. Second, it shows that the parametrization developed by [1] produces results consistent with in-situ measurements in HIWC environment. Third, it shows a potential for lidar-only IWC retrievals in the future once the inherent uncertainties in lidar data processing are accounted for.

ACKNOWLEDGEMENTS

Funding for the NRC Convair-580 participation in the HAIC-HIWC field project was provided by NRC and ECCC. We would like to acknowledge the NRC and ECCC project crew that supported the field project. We also acknowledge the staff at Alpenglow Inc. for their technical support.

References

- [1] Heymsfield, A. et al, 2014, Relationships between Ice Water Content and Volume Extinction Coefficient from In Situ Observations for Temperatures from 0° to -86°C : Implications for Spaceborne Lidar Retrievals *J. Appl. Meteor. Climatol.*, 53, 479–505, doi: 10.1175/JAMC-D-13-087.1.
- [2] M. L. Grzych and J. G. Mason, Conditions Associated with Jet Engine Power Loss and Damage Due to Ingestion of Ice Particles: What We've Learned Through 2009 14th Conf. Aviat. Range, *Aerosp. Meteorol.*, 2010.
- [3] Wendisch M., J.L. Brenguier, 2013: Airborne Measurements for Environmental Research: Methods and Instruments. Willey, 641p.
- [4] Davison, C. R. et al, 2012, Naturally Aspirating Isokinetic Total Water Content Probe: Pre-flight Wind Tunnel Testing and Design Modifications AIAA Paper 2012-3040, 4th Atmospheric and Space Environments Conference, 25 - 28 June 2012, New Orleans, Louisiana.
- [5] Sasano, Y. et al, 1979, Geometrical form factor in the laser radar equation: an experimental determination *Appl. Opt.* 18, 3908-3910.
- [6] Wolde, M. and Pazmany, A., 2005, NRC Dual-Frequency Airborne Radar For Atmospheric Research, Proc. 32nd Conf. on Radar Meteorology, Albuquerque, USA.
- [7] Leroy, D. et al., 2016, HAIC/HIWC field campaigns - Specific findings on ice crystals characteristics in high ice water content cloud regions", 8th AIAA Atm. and Space Env. Conf., AIAA 2016-4056.